University of Central Florida

STARS

2020

Non-Alcoholic Fatty Liver Disease and the Gut Microbiome: The Effects of Gut Microbial Metabolites on NAFLD Progression in a 2-Organ Human-on-a-Chip Model

Rachel H. Boone
University of Central Florida

Part of the Microbiology Commons

Find similar works at: https://stars.library.ucf.edu/honorstheses

University of Central Florida Libraries http://library.ucf.edu

Recommended Citation

NON-ALCOHOLIC FATTY LIVER DISEASE AND THE GUT MICROBIOME: THE EFFECTS OF GUT MICROBIAL METABOLITES ON NAFLD PROGRESSION IN A 2-ORGAN HUMAN-ON-A-CHIP MODEL

by

RACHEL H. BOONE

A thesis submitted in partial fulfilment of the requirements
for the Honors Undergraduate Thesis Program in Biomedical Sciences
in the College of Medicine
and in the Burnett Honors College
at the University of Central Florida
Orlando, Florida

Spring Term
2020

Thesis Chair: Dr. James J. Hickman, Ph.D.

ABSTRACT

Using a novel, adipose-liver, two-organ, human-on-a-chip system, the metabolic disease non-alcoholic fatty liver disease was modeled. This model was then used to test the effects of the gut microbiome on NAFLD progression. Two products of the gut microbiome, Trimethylamine-n-oxide and butyrate, were selected as representatives of potentially harmful and potentially beneficial compounds. A dose response, adipocyte and hepatocyte monocultures controls, and HoaC systems were run for 14 days. Through this experimentation, it was found that a dysbiosis of the gut microbiome could be influencing NAFLD progression. Additionally, further development and discovery regarding adipose-liver systems was added to the ongoing conversation of HoaC systems and their usages.

ACKNOWLEDGMENTS

TABLE OF CONTENTS

LIST OF TABLES

LIST OF FIGURES

CHAPTER 1: INTRODUCTION

NAFLD and Its Progression

Non-alcoholic fatty liver disease (NAFLD) is a metabolic disease highly correlated with type 2 diabetes mellites and obesity. It is characterized by the accumulation of fat, in the form of triglycerides, in the liver (hepatic steatosis). NAFLD can progress to disease states such as non-alcoholic Steatohepatitis (NASH), fibrosis, cirrhosis, and liver cancer [1, 2]. This is especially concerning considering that NAFLD is becoming more prevalent in the United States, with rates being reported as high as 46% [3]. NASH and cirrhosis due to NAFLD are increasing in frequency as indications for liver transplantation, with NASH already being the third most common indication in the United States [2-4].

A "multiple hit hypothesis" has been developed to describe NAFLD progression. This hypothesis asserts that excess free fatty acids (FFA), insulin resistance (IR), adipocyte dysfunction, and dysbiosis (an imbalance in the population of the gut microbiome (GM)), along with genetic, epigenetic, and dietary factors can all contribute to liver steatosis [1, 5].

Triglycerides, which are formed by the esterification of FFAs, are normally stored briefly in the liver, but high-fat diets, obesity, and IR resistance can increase the FFA concentration and lead to lipotoxicity. IR resistance can increase the storage of triglycerides through two main mechanisms: in adipocytes, IR can lead to the impaired inhibition of lipolysis, and IR in hepatocytes increases hepatic de novo lipogenesis. [1, 6, 7].

In addition to increasing FFA levels, obesity and IR can lead to the dysfunction of adipokine secretion. Adipokines, such as leptin and adiponectin, are hormones secreted by adipose tissue. Leptin is an adipokine involved in the prevention of lipid storage in non-

adipocyte tissue and has pro-inflammatory properties. Obesity leads to an upregulation in plasma leptin concentration, causing the body to grow resistant to leptin's latter effects while still being susceptible to the former. Adiponectin is an anti-inflammatory adipokine which can also improve IR and has an anti-fibrotic effect. However, adiponectin is downregulated in obesity. Thus, the dysfunction of adipokine secretion, caused by disease states such as obesity, can play a major part in the development of hepatic steatosis and the progression of NAFLD [1, 7, 8].

Hepatic inflammation through the JNK-AP-1 and IKK-NF-κB pathways can also drive NAFLD pathogenesis [9, 10]. Adipocytes contribute to low grade inflammation with the production of IL-6 and TNF-α [8, 9]. When there is adipocyte damage or an increase in adipose tissue volume, such as in obesity, the secretion of these compounds is upregulated [10]. Similarly, hepatic tissue damage can increase the inflammatory response. Finally, endotoxins and other pathogen-associated molecular patterns (PAMPS) produced by the GM can make their way into the liver through a "leaky gut" and they can initiate inflammation through Toll-like receptors [1, 11].

The Gut Microbiome

The gut microbiome consists of the fungi, viruses, and the roughly 3.9×10^{13} bacteria, belonging to thousands of operational taxonomic units, which live in the human colon [11, 12]. The GM plays an active role in the health of the host, producing many metabolic products and signaling molecules. These products include metabolites such as bile acids, choline derivatives, short chain fatty acids (SCFAs), alcohols, and endotoxins, which can have a range of effects on the host [1, 5, 13].

In recent years, the effects of gut microbial compounds on humans has been an area of interest in the research community. There is strong evidence that GM can influence mental health and disorders such as major depressive disorder [14]. Similarly, higher concentrations of trimethylamine-n-oxide (TMAO), which is produced by the GM, has been identified as a risk factor for strokes, and the dysbiosis in the GM has been associated with cardiovascular disease development [15]. When it comes to NAFLD, problems with the GM is one of the main "hits" in the multiple hit hypothesis. While NAFLD and NASH are often associated with metabolic problems like obesity or high caloric diets, NAFLD is also present in patients who do not present with other diseases like obesity, and it is hypothesized that the GM could be responsible for these cases [16].

Although studies differ in exact results, they show that the microbial population is often different between healthy individuals and those with NAFLD, and they most commonly show differences in the population of Bacteroidetes and Firmicutes [17]. It has also been observed that healthy patients have more bacteria from the phyla Bacteroidetes and a more diverse gut population than individuals with NAFLD [18]. The change in gut population is one of the main reasons why dysbiosis of the GM is believed to be a major driver of NAFLD, especially in patients without other disease states [16].

There are a number of ways in which dysbiosis could be influencing liver health. The first way is by the introduction of endotoxin and other compounds to the liver through a leaky gut. In a healthy colon, the epithelial cells form a tight barrier which bacteria and their products are unable to cross unless transported. However, in certain disease states such as chronic inflammation, or even high rates of alcohol production by microbes due to dysbiosis in the GM,

the gut enterocytes can become damaged and this barrier can become permeable to compounds such as endotoxin (lipopolysaccharide, LPS), which is produced by Gram negative bacteria as part of their cell walls. LPS, as well as other PAMPS, can then cause inflammation through activation of Toll-like receptors [1, 5, 11, 17].

Additionally, the low choline levels in the liver, due to poor diet or microbial metabolization of choline into trimethylamine (TMA), can promote liver damage and NAFLD [17, 19]. Bile acids' pool size and composition can influence liver health and is regulated in part by the GM [17, 20]. The digestion and metabolism of starch and non-starch polysaccharides by microbes into short chain fatty acids (SCFAs) account for a significant portion of energy adsorption by humans. It is hypothesized that a change in the population of the GM to favor the microbes that produce more SCFAs could increase this energy production and lead to obesity [1, 21].

Changes in the microbial population could be causing the concentrations of other metabolites to be altered as well. Many of these metabolites, such as TMAO and butyrate, could have direct interactions with hepatic tissue, and thus an alteration in their concentration could be influencing hepatic health [13, 17].

TMAO is a derivative of choline. Humans consume choline and the gut microbes metabolize the dietary choline into trimethylamine (TMA) as well as other products [19]. TMA is then absorbed by the gut and is transported to the liver where it is further metabolized by hepatocytes into TMAO [15]. TMAO is a proinflammatory molecule previously associated with cardiovascular disease and NAFLD [13, 15, 22]. In addition to possibly inducing inflammation, TMAO has been shown to modulate reverse cholesterol transport and sterol metabolism [23].

Butyrate is a SCFA produced by gut microbes shown to be absorbed by the gastrointestinal tract and transported to the liver [24]. In addition to affecting the health of intestinal epithelial cells, butyrate has anti-inflammatory properties through the inhibition of NF-κB [25]. In mouse models, butyrate has also been shown to improve insulin signaling [26]. If dysbiosis of the GM can drive changes in the concentration of potentially beneficial compounds like butyrate or harmful compounds like TMAO, the pathogenesis of NAFLD could be promoted.

Disease Models

Today, science relies heavily on animal models, primarily rodent models, to model human diseases. These animals act as surrogates for humans for the testing of new drugs or to model diseases. Although these models have made major advances in medicine possible, there are also limitations to their utility. Animal behavior and physiology can be impacted by laboratory conditions that result in stress for the animals including repeated handling. Additionally, the physiology and genetics of animal models as well as the pathology of animal disease models is not identical to humans and human diseases and thus presents differently between the species. The difference between animal models and humans is so great that around 90 percent of drugs which pass in animal testing fail to be effective in humans due to toxicity issues [27, 28]. Another objection to the use of animal models is the question of ethics. Despite the limitations of animal models, as of 2005 more than 115 million animals were used annually in the biomedical industry [29].

As an alternative to traditional animal models, human-on-a-chip (HoaC) microphysiological systems have been developed. These systems consist of human primary or

stem cell-derived cells organized into functional "organs" which share feeding medium, dosed drugs, and metabolites through the microfluidic system housing. HoaC systems combine biomedical sciences with the fields of engineering and chemistry to create *in vitro* models which contain relevant human cell types, limited variability, and the ability to obtain both functional and molecular readouts of not only the target pathway but also the peripheral effects while avoiding animal testing and allowing for more complexity than traditional 2-D models would provide [30-33]. HoaC systems also allow for phenotypic drug discovery (PDD) as opposed to target-based drug discovery (TDD). While most drug testing today requires TDD, where knowledge or a hypothesis as to what effects a drug may have is needed beforehand, PDD offers the ability to determine the effects of a drug outside the limited predicted effects [34]. Already, HoaC systems have been created to emulate the blood brain barrier, lung, heart, intestine and many more organ systems including larger, more complex systems such as a four organ model containing cardiac, muscle, neuronal, and liver modules [30, 32].

CHAPTER 2: MEDIA FORMULATION

A serum free, defined medium, described in previous studies, was used as the base for each condition's respective medium [32]. The Blood Memetic Medium (BMM) was modified for this study with a change in glucose and insulin concentrations. Additionally, Neurobasal-A medium -D-glucose, - sodium pyruvate (Life Technologies, A24775-01) 1x B27 – insulin (Life Technologies, A1895601), and 0.22mM sodium pyruvate (Sigma, S8636) were used. This change was used to create more physiologically relevant conditions to NAFLD so that the control medium (healthy, h, hBMM) contained significantly less glucose and insulin, while the diabetic condition (+d, dBMM) had a higher concentration of glucose and insulin.

Since there are several disease states which have been shown to correlate if not contribute to the pathogenesis of NAFLD, multiple conditions were emulated through the addition of factors to the medium. These media formulations were designed to mimic the serum of a patient with the specified health condition. The healthy condition was the base BMM. The diabetic condition had higher concentrations of glucose and insulin. The supplementation of the FFAs BSA-conjugated palmitate (Sigma, A8806) and oleate (Sigma, O3880) characterized the obese condition (+lipids, hBMMlipids). The condition emulating an inflamed state (+TNF-α, +TNF, hBMMTNF) was supplemented with the cytokine TNF-α (Sigma, T0157). The last condition was the diabetic, inflamed, and obese condition (dBMMTNFlipids). [35]

TABLE 1: BLOOD MEMETIC MEDIA CONDITION COMPOSITION			
Condition	**Condition Abbreviation**	**Added Factors**		**Concentration of Condition Factors**
Healthy	h hBMM	Glucose	5mM
		Insulin	1nM
		Palmitate	0M
		Oleate	0M
		TNF-α	0M
Diabetic	+d dBMM	Glucose	25mM
		Insulin	69μM
		Palmitate	0M
		Oleate	0M
		TNF-α	0M
Inflammation	+TNF-α +TNF hBMMTNF	Glucose	5mM
		Insulin	1nM
		Palmitate	0M
		Oleate	0M
		TNF-α	10μM
Obese	+lipids hBMMTNFlipids	Glucose	5mM
		Insulin	1nM
		Palmitate	45μM
		Oleate	65μM
		TNF-α	0M
Inflamed, Obese, and Diabetic	dBMMTNFlipids	Glucose	25mM
		Insulin	69μM
		Palmitate	45μM
		Oleate	65μM
		TNF-α	10μM

CHAPTER 3: DOSE RESPONSE

Purpose

In an *in vitro* study, the physiological concentration of the chosen microbial metabolites, TMAO and butyrate, may not be significant enough to cause a measurable effect over the course of a 14 day dosing, and thus a dose response was performed to determine the appropriate concentration of TMAO and butyrate for *in vitro* testing. The goal was to find a concentration which would produce *in vitro* changes in steatosis but was not so concentrated as to lose physiological relevance or cause cell death.

Cell Culture

For the dose response, human hepatocellular carcinoma (HepG2/C3A) (ATCC® CRL-10741™) cells were used. This line of cells was used for this preliminary data because of their ease of culture and low cost. HepG2 cells were plated on 15mm diameter round glass coverslips, sterilized in 70% isopropyl alcohol (IPA) and allowed to dry, at a plating density of 6×104 cells per coverslip in Dulbecco's Modified Eagle Medium (DMEM). The following day, the cells were moved to BMM +/- d and +/- lipids conditions and varying concentrations of TMAO or butyrate. The cultures were fed and dosed regularly over the course of 14 days.

Steatosis

The cells were washed with phosphate buffered saline (PBS) and then fixed using 4% paraformaldehyde (PFA) for 10 minutes at room temperature. After another wash with PBS, the coverslips were covered with a 3:2 Oil Red O dye (Sigma, O1391) to deionized water (diH$_2$O) solution for 30 minutes at room temperature. Additional washes with PBS were used to remove the excess dye and precipitate. The cells were then imaged at 100x using a phase microscope. Oil

Red O is a lipid soluble dye which stains lipids a deep red color. Thus, an increase of red in the images correlates to an increase in the fat being stored by the cells, an increase in steatosis. For the dose response, the steatosis was not quantified but was analyzed qualitatively along with the general health of the cultures.

Results

As expected, the dBMM conditions had more steatosis than their respective hBMM controls. Similarly, the +lipids conditions had more steatosis than their respective -lipids controls. These results indicated that the hepatocytes do store different levels of lipids based on the condition. They also show that the +d and +lipids conditions induced an increase in steatosis as they theoretically should.

The +1μM TMAO conditions did not appear to store more lipids than their respective controls. The +100μM TMAO conditions showed an increase in lipid storage compared to their respective controls. However, this concentration of TMAO seemed to cause some cell death. Based on these results and the concentration of TMAO found in the literature, the concentration of 10μM TMAO was chosen as the dosing concentration for the remainder of study.

Both the +1nM butyrate and +1μM butyrate conditions had less steatosis than their respective controls. The +1mM butyrate conditions had more steatosis than their respective controls. This switch from storing less lipids to storing more lipids with an increase in concentration of butyrate is most likely caused by the fact that butyrate both has anti-inflammatory properties and can act as a source of energy. It is possible that the great excess of energy in the form of butyrate in the +1mM butyrate conditions caused a greater effect than the signaling of butyrate could. It was thus concluded that a dosing concentration closer to the lower

two was desired. Based on these results and the literature, a concentration of 10μM butyrate was chosen as the dosing concentration for the remainder of the study.
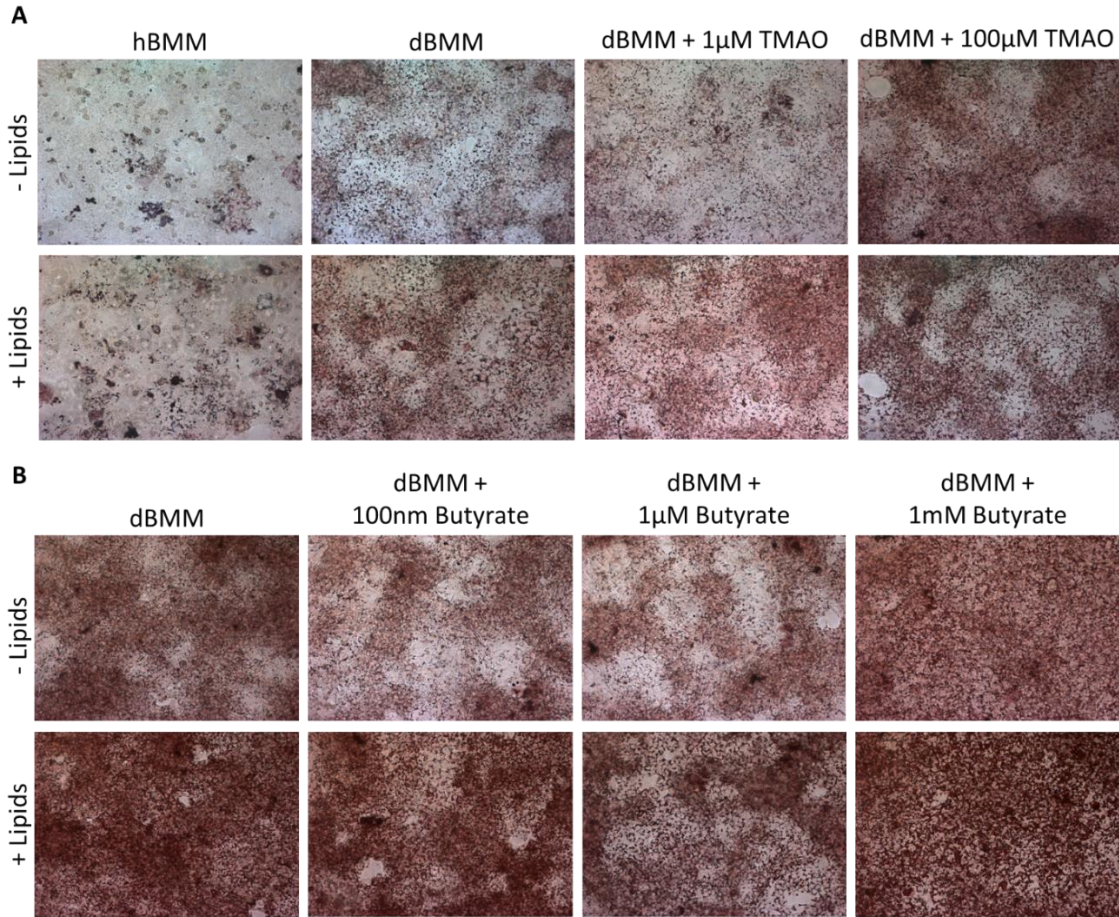
FIGURE 1: Dose Response to TMAO and Butyrate.
*(**A**) HepG2 cells were fed for 14 days with hBMM, hBMMlipids, dBMM, dBMMlipids, dBMM+1μM TMAO, dBMMlipids+1μM TMAO, dBMM+100μM TMAO, and dBMMlipids+100μM TMAO. The cells were fixed with 4% PFA and stained with Oil Red O dye. Images were taken at 100X on a phase microscope. (**B**) HepG2 cells were fed for 14 days with dBMM, dBMMlipids, dBMM+100nm butyrate, dBMMlipids+100nm butyrate, dBMM+1μM butyrate, dBMMlipids+1μM butyrate, dBMM+1mM butyrate, and dBMMlipids+1mM butyrate. The cells were fixed with 4% PFA and stained with Oil Red O dye. Images were taken at 100X on a phase microscope*

. TABLE 2: DOSE RESPONSE TO TMAO AND BUTYRATE SUMMARIZED			
	<10μM	**10μM**	**>10μM**
TMAO	Limited Effect	Visible Increase in Steatosis	Cell Death
Butyrate	Limited Effect	Visible Decrease in Steatosis	Visible Increase in Steatosis

CHAPTER 4: CELL CULTURE AND ASSAY METHODOLOGY

Cell Culture

Primary hepatocytes from Massachusetts General Hospital (MGH) (Lot# 54.1) were plated on 15mm coverslips at a cell density of approximately 250,000 cells/cs in vendor recommended medium. The coverslips were prepared by sterilization in 70% IPA and then incubated with ECL Cell Attachment Matrix (Millipore Sigma, 08-110) diluted in PBS for 1 hour, then washed with PBS. The cells were then allowed to recover, being fed regularly, for 5-9 days.

Primary human cardiac preadipocytes (Cell Applications, Sigma, No. 802H-05A) were plated on 15mm coverslips at a cell density of approximately 90,000 cells/cs. The cells were allowed to grow to confluency and recover for 24-48 hours. Human Preadipocyte Growth Medium (Cell Applications, Sigma, 811-500) was used for both the plating and the recovery. After the preadipocytes had grown confluent, they were moved to Human Adipocyte Differentiation Medium (Cell Applications, Sigma, 811D-250) and allowed to differentiate, being fed regularly, for 12-16 days.

After the cells had recovered and differentiated, they were moved to BMM conditions +/- 10μM TMAO or Butyrate. They were fed and dosed regularly for 14 days. Alternatively, the coverslips were assembled into adipose-liver (A-L) systems and allowed to recover in hBMM for 16-24 hours before being dosed with BMM conditions +/- TMAO or Butyrate for 13-14 days.

HoaC Systems

A two-organ HoaC system was used to model NAFLD in these experiments. The systems themselves consisted of a top and a bottom gasket between a top and a bottom housing fastened

with screws. The housings and gaskets were designed to form two wells for 15mm coverslips (one for the white adipose tissue (WAT) module and one for the liver module), two access ports, and a channel connecting the modules and access ports.

Before assembly, the systems were cleaned with 1% tergazyme 48 hours prior to assembly and all components were sterilized in 70% IPA and dried fully. In response to toxicity issues, a more thorough cleaning was done by sonicating in 1% tergazyme 3x 30 minutes and in deionized water 3x 30 minutes followed by sterilization.

To assemble, 1ml of hBMM was added to the bottom housing+gasket. The coverslips were then transferred to their appropriate wells cell side up. The top housing+gasket was secured, and the access ports filled with hBMM so that total medium volume was roughly 1.5ml. The systems were stored on a rocker with a 1° tilt to allow the medium to flow between the modules.
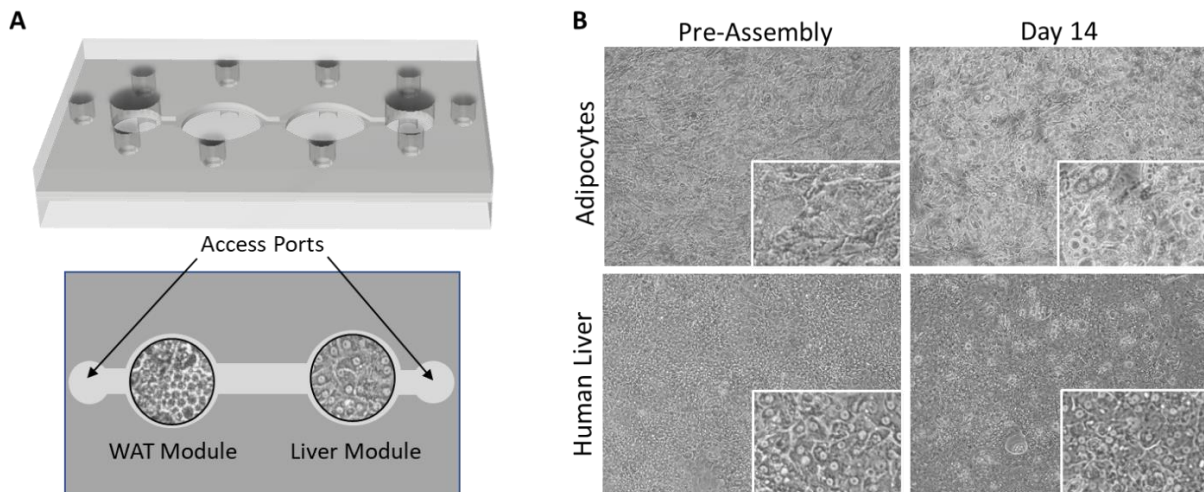

FIGURE 2: Adipose-Liver Systems Design.
(A) Schematic of the two-organ adipose-liver *systems. The systems consist of two access ports, two wells for the organ modules, and a channel connecting them. (B) The liver and white adipose tissue modules before system assembly and after 14 days. Images taken at 100X and 200X using a phase microscope.*

Hepatic Steatosis

To determine the amount of steatosis in each condition, the hepatocytes were stained with Oil Red O dye as done in the dose response. The coverslips were them imaged at 100X and 200X using a phase microscope. Several 200X images were taken of each condition and then processed using the image processing software ImageJ [36]. Images were converted to 8-bit, the threshold was set so that background was removed, and the setting "Watershed" was turned on to separate particles. The setting "Black Background" under both the "Image>Adjust>Threshold" and "Process>Binary>Options" tabs was unselected. This produced images which were pixelated and binary with the red stain in black and the background in white. The %Area of the black in the images was then recorded. Places of low cell confluency or high debris were avoided for quantification. %Area was average for each condition and normalized to the Average %Area of the Healthy control condition.
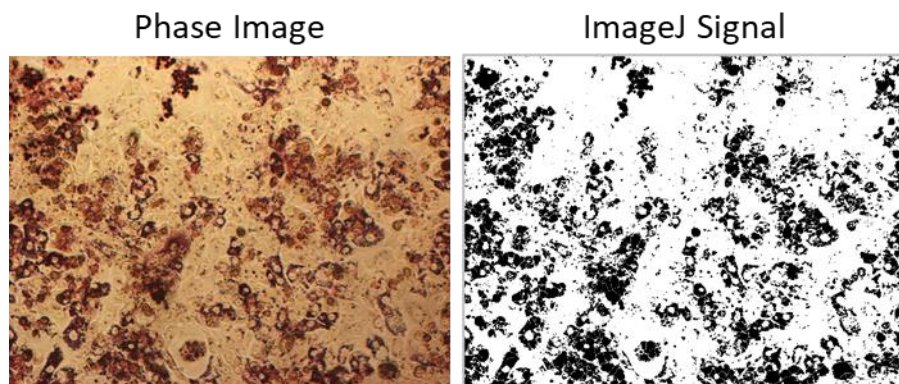
FIGURE 3: Quantification of Steatosis Using ImageJ.
Hepatic cells stained with Oil Red O were imaged under a phase microscope at 200X. The image processing software, ImageJ, was used to convert the image into a pixelated, black and white version which could be quantified by taking the %Area.

Hepatic Enzyme Activity

The activity of the enzyme CYP3A4 was measured as an indicator of liver function. This was done with the P450-Glo™ CYP3A4 Assay and Screening System (Promega, V900). In the

first reaction of this assay the CYP3A4 enzyme in the hepatocytes metabolizes the Luciferin-IPA reagent into luciferin. In the second reaction, a luciferase enzyme metabolizes luciferin and produces light as one of the products.

On the endpoint day of dosing, the hepatocytes were washed with PBS to remove the phenol red, and were moved to a 24 well plate. 180ul of a 12μM solution of the Lucifern-IPA diluted in DMEM -phenol red (ThermoFisher, 11054020) was added to each well. After an hour of incubation, the solution was removed and stored at -20°C. 50μL of each sample, standard, and blank were added to a white, opaque, 96 well plate. 50μL of the Luciferin Detection Reagent was added to each well and incubated for 20 minutes in the dark. The luminescence was measured using a plate reader.

Adipocyte Cytokine Secretion

To determine the effects of the conditions on adipokine secretion, the production of leptin and adiponectin was measured using an enzyme-linked immunosorbent assay (ELIZA). At day 14, the medium from each condition was collected and stored at -20°C. The Human Leptin ELISA Kit (Abcam, ab179884) and Human Adiponectin ELISA Kit (Abcam, ab9996) were then used to assay the collected medium.

Adipocyte Insulin Resistance

The presence, or lack thereof, of GLUT-4 and insulin receptor were used as indications of insulin resistance. Immunocytochemistry (ICC) was used to measure the presence of these two markers. On day 14, the adipocyte coverslips were washed with PBS and fixed using 4% PFA for 10 minutes. After being washed twice more with PBS, the coverslips were incubated in blocking buffer consisting of PBS + 1% Bovine Serum Albumin (BSA) and 5% Fetal Bovine

Serum (FBS) for one hour. Rabbit anti-α-insulin receptor antibody, β subunit (Sigma, 07-724) was used to detect insulin receptor and mouse anti-GLUT4 antibody (Invitrogen, MA5-17176) was used for the detection of GLUT-4. A 1:1000 dilution of these antibodies in the blocking buffer was made and the adipocytes were incubated in this solution overnight at 4°C. They were then washed with PBS and incubated in the dark for 2 hours at room temperature in a 1:1000 solution of the secondary antibodies, Donkey anti-Mouse IgG Alexa Fluor 488 (Invitrogen, A21202) and Goat anti-Rabbit IgG Alexa Fluor 568 (Invitrogen, A11036), and the blocking buffer. They were then washed 3x 5 minutes with PBS and stained with a solution of 4′,6-diamidino-2-phenylindole (DAPI) for 5 minutes in the dark at room temperature. After another 3x 5 minutes washes with PBS, the coverslips were mounted onto glass slides using ProLong Diamond Antifade Mountant (Invitrogen, P36970), set to dry in the dark overnight, and stored in the dark at 4°C until imaged at 200X on a confocal microscope.

To quantify the amount of GLUT-4 and insulin receptor being expressed, the images were processed using the ImageJ software. The images (in Tiff format) were separated using the "Images>Stacks>Stacks to Images" setting. The Mean Grey Values of 488 and 568 images (green and red, GLUT-4 and insulin receptor) were then measured.

CHAPTER 5: MONOCULTURE RESULTS

Culture Health

Hepatocytes in the BMM proved to be viable up to 14 days in monoculture. The exception to this were the hBMMtnf conditions which showed significant cell death. The conditions using dBMM +/- other factors appeared to have more confluency. This is likely due to the energy source, glucose, having a higher concentration and thus being more readily available for the cells in these conditions.

The monoculture hepatocytes dosed with +/- butyrate were cut off at 7 days to better reflect the+/- butyrate adipose-liver systems. All conditions appeared confluent and healthy at 7 days. The cultures cut off at 7 days appeared to be more confluent than the 14-day cultures.
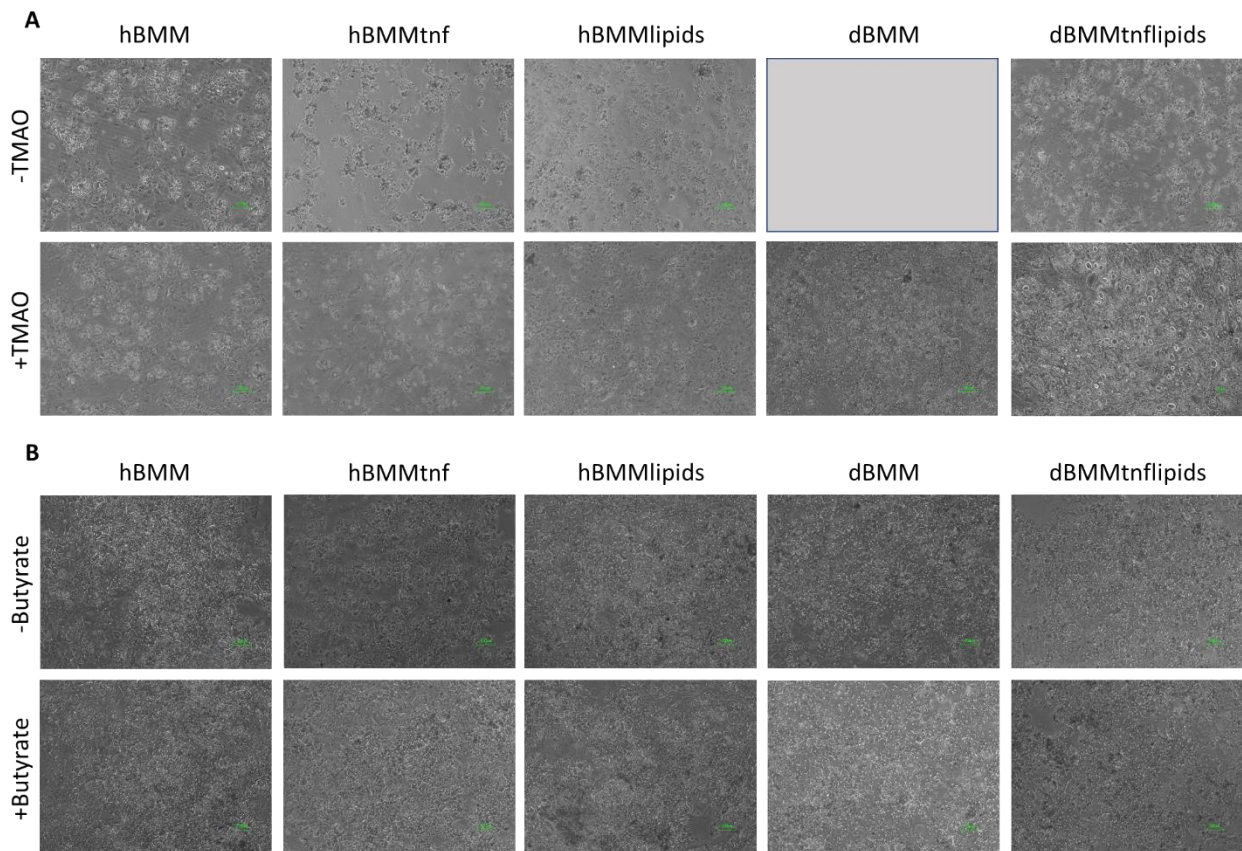
FIGURE 4: Cell Health of Hepatocytes in Monoculture.
*(**A**) MGH hepatocytes were fed for 14 days with hBMM, hBMMtnf, hBMMlipids, dBMM, dBMMtnflipids +/- 10μM TMAO. The condition dBMM was not included. The cells were imaged at 100X using a phase microscope. (**B**) MGH hepatocytes were fed for 14 days with hBMM, hBMMtnf, hBMMlipids, dBMM, dBMMtnflipids +/- 10μM butyrate. Images were taken at 100X on a phase microscope.*

Adipocytes in the BMM were viable and confluent through 14 days. This was independent of condition. All conditions also showed proper morphology and stored lipids. Qualitatively, the hBMMtnf +/- TMAO/Butyrate conditions stored less lipids than the other conditions, which may speak to the health of the cells.

A

B
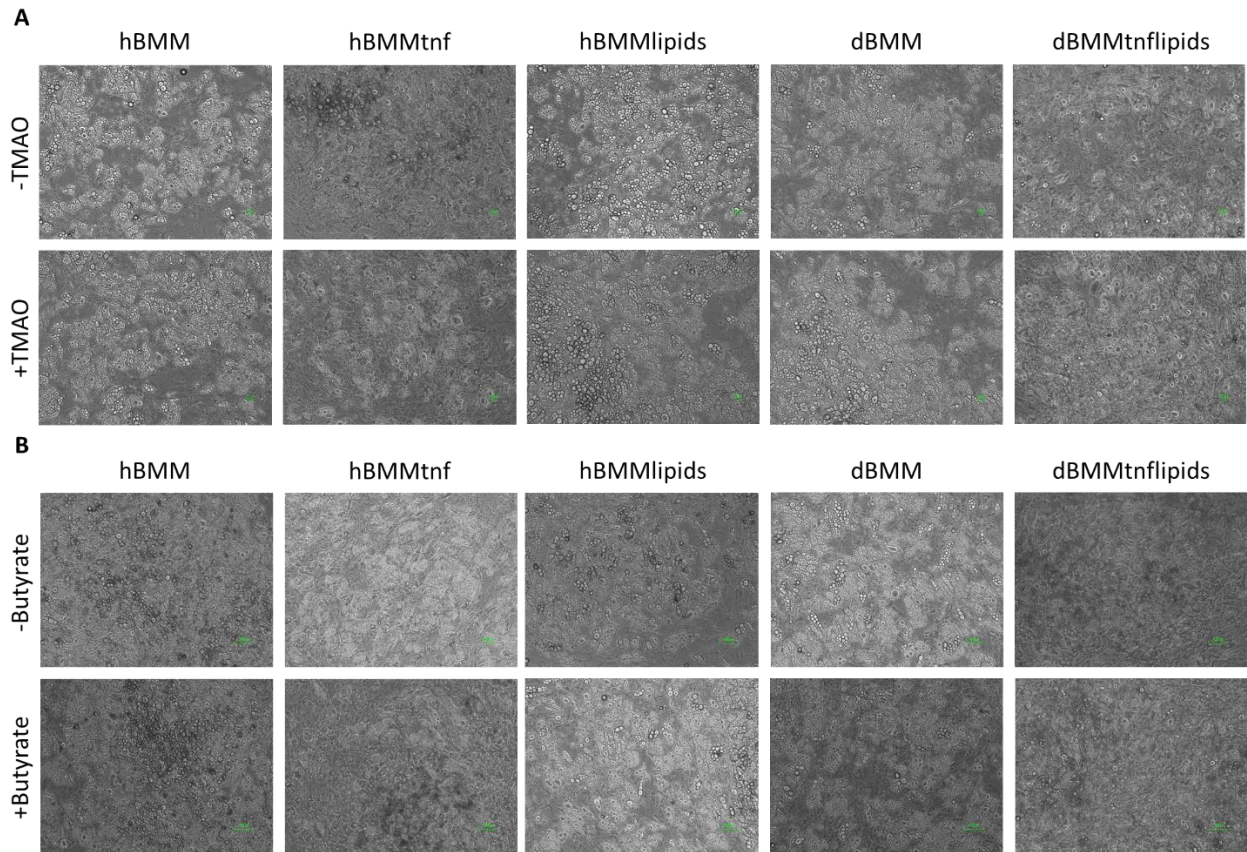
FIGURE 5: Cell Health of Adipocytes in Monoculture.
*(**A**) Adipocytes were fed for 14 days with hBMM, hBMMtnf, hBMMlipids, dBMM, dBMMtnflipids +/- 10µM TMAO. The cells were imaged at 100X using a phase microscope. (**B**) Adipocytes were fed for 14 days with hBMM, hBMMtnf, hBMMlipids, dBMM, dBMMtnflipids +/- 10µM butyrate. Images were taken at 100X on a phase microscope.*

Hepatic Steatosis

As expected, the hBMMlipids, dBMM, and dBMMtnflipids +/- TMAO conditions were all higher in steatosis than the hBMM +/- TMAO conditions in hepatocyte monoculture when dosed for 14 days. Because of the poor morphology of the hBMMtnf +/- TMAO conditions, they were not included in the quantification. Very little change was observed between the -TMAO and +TMAO conditions and results remain inconclusive at this time.

As expected, the hBMMlipids, dBMM, and dBMMtnflipids +/- Butyrate conditions were also higher than the hBMM +/- Butyrate conditions in the hepatocytes dosed for 7 days in

monoculture. Dosing with butyrate worsened the steatosis in hBMM and hBMMtnf while it

improved steatosis in dBMM+/-lipids.
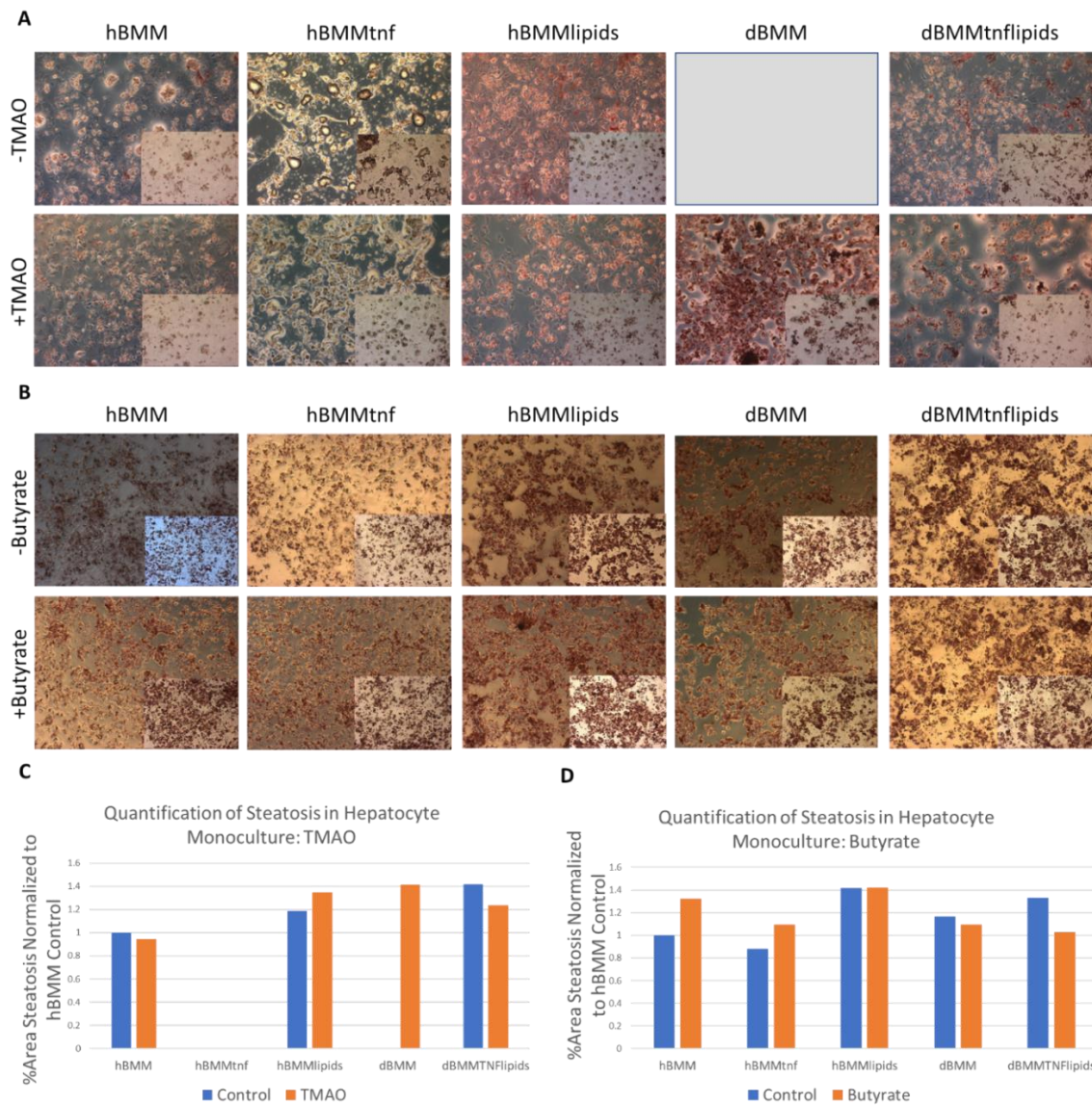
FIGURE 6: Steatosis of Hepatocytes in Monoculture.
(*A*) *MGH hepatocytes were fed for 14 days with hBMM, hBMMtnf, hBMMlipids, dBMM, dBMMtnflipids +/- 10µM TMAO. The condition dBMM was not included. The cells were fixed with 4% PFA and stain with Oil Red O dye. The cells were imaged at 100X and 200X using a phase microscope. (B) MGH hepatocytes were fed for 14 days with hBMM, hBMMtnf, hBMMlipids, dBMM, dBMMtnflipids +/- 10µM butyrate. The cells were fixed with 4% PFA and stain with Oil Red O dye. Images were taken at 100X and 200X on a phase microscope. (C) The steatosis expressed in monoculture hepatocytes +/- TMAO was quantified by taking the %Area of the 200X images using the ImageJ software. The %Area was normalized to the hBMM control. N=1 for all conditions except hBMMtnf +/- TMAO and dBMM which were not included. (D) The steatosis expressed in monoculture hepatocytes +/- Butyrate was quantified by taking the %Area of the 200X images using the ImageJ software. The %Area was normalized to the hBMM control. N=1 for all conditions.*

21

Hepatic Enzyme Activity

The most prominent result from the CYP3A4 assay was that the conditions with +TNF had almost no activity. In the conditions of hBMMtnf +/- TMAO, this was not surprising considering the poor health of the cells, but this result was seen in the other +TNF conditions as well. In the +/-TMAO cultures which were taken to 14 days, the hBMMlipids and dBMM +/- TMAO were higher than the hBMM conditions, while the +/- Butyrate conditions, which were cultured for 7 days, demonstrated the opposite pattern. It is also uncertain why the activity of the +/- Butyrate monocultures had such higher activity levels than any other culture with as high as 60-fold+ more activity.
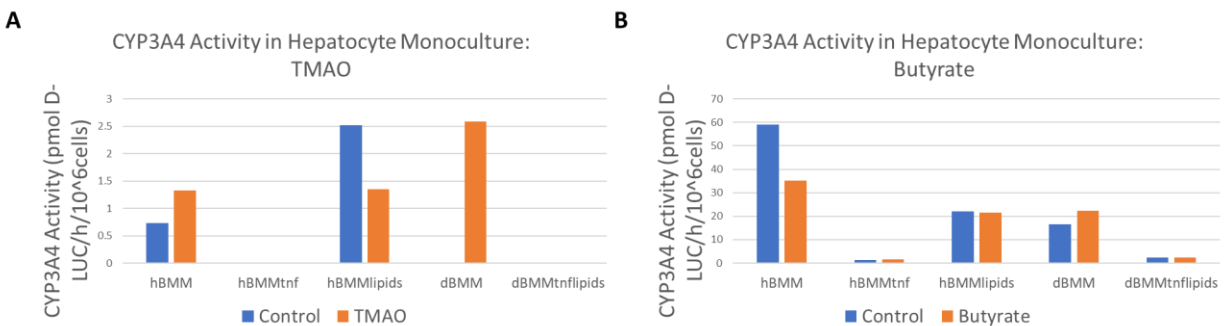

FIGURE 7: CYP3A4 Activity of Hepatocytes in Monoculture.
(A) Hepatocytes were fed for 14 days with hBMM, hBMMtnf, hBMMlipids, dBMM, dBMMtnflipids +/- 10μM TMAO. On day 14, the CYP3A4 activity of the cultures was measured. N=1 for all conditions except dBMM which was not included. (B) Hepatocytes were fed for 7 days with hBMM, hBMMtnf, hBMMlipids, dBMM, dBMMtnflipids +/- 10μM Butyrate. On day 7, the CYP3A4 activity of the cultures was measured. N=1 for all conditions.

Adipocyte Cytokine Secretion and Insulin Resistance

Limited patterns were observed regarding the secretion of leptin and adiponectin in monoculture. Additional replicates are needed. GLUT-4 and insulin receptor expression was increased with the dosing of TMAO in monoculture in most conditions. The opposite was observed for butyrate which appeared to lower GLUT-4 and insulin receptor expression. In

monoculture the expression of GLUT-4 and insulin receptor was increased in the more diseased
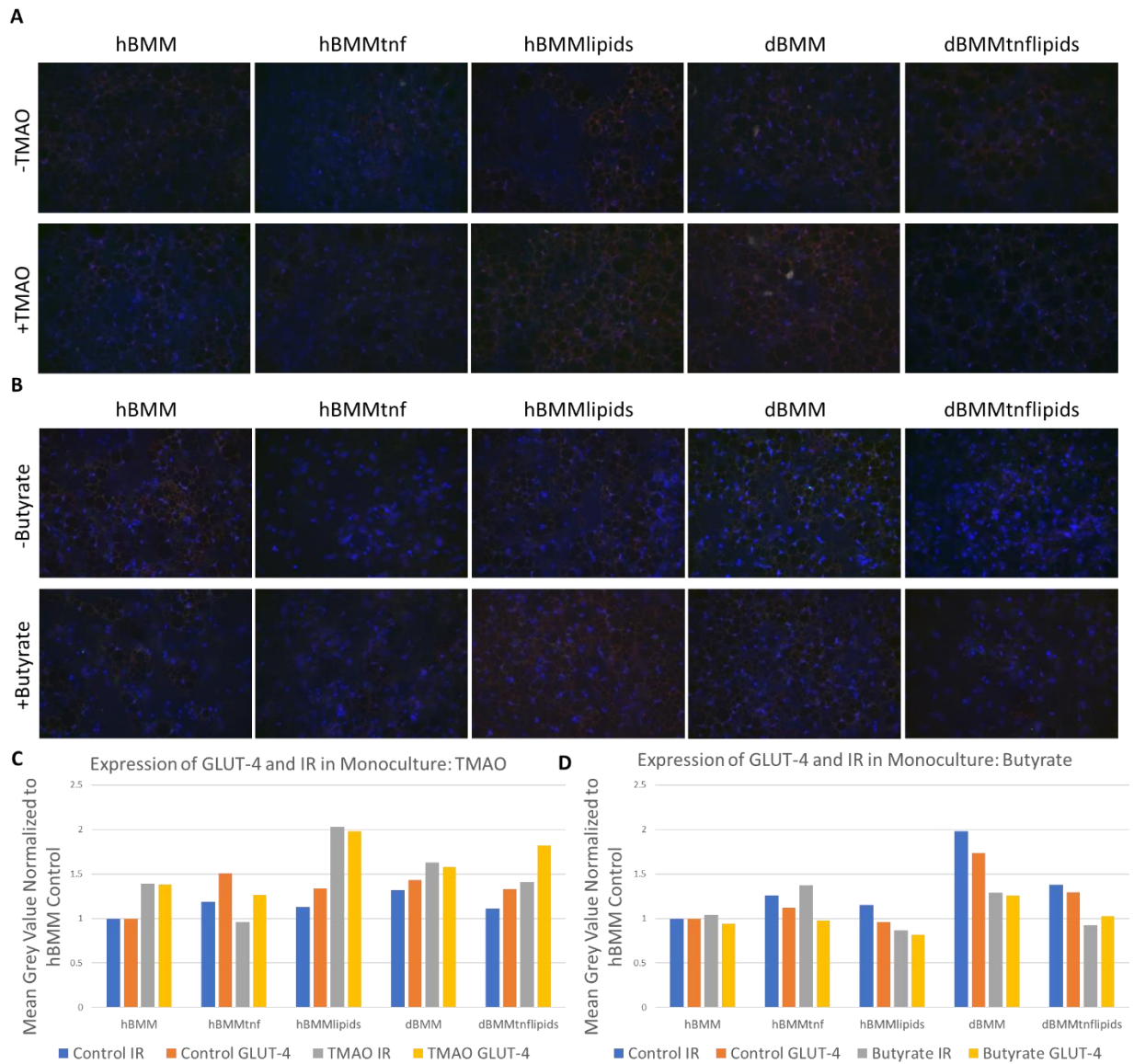
states when compared to hBMM control.
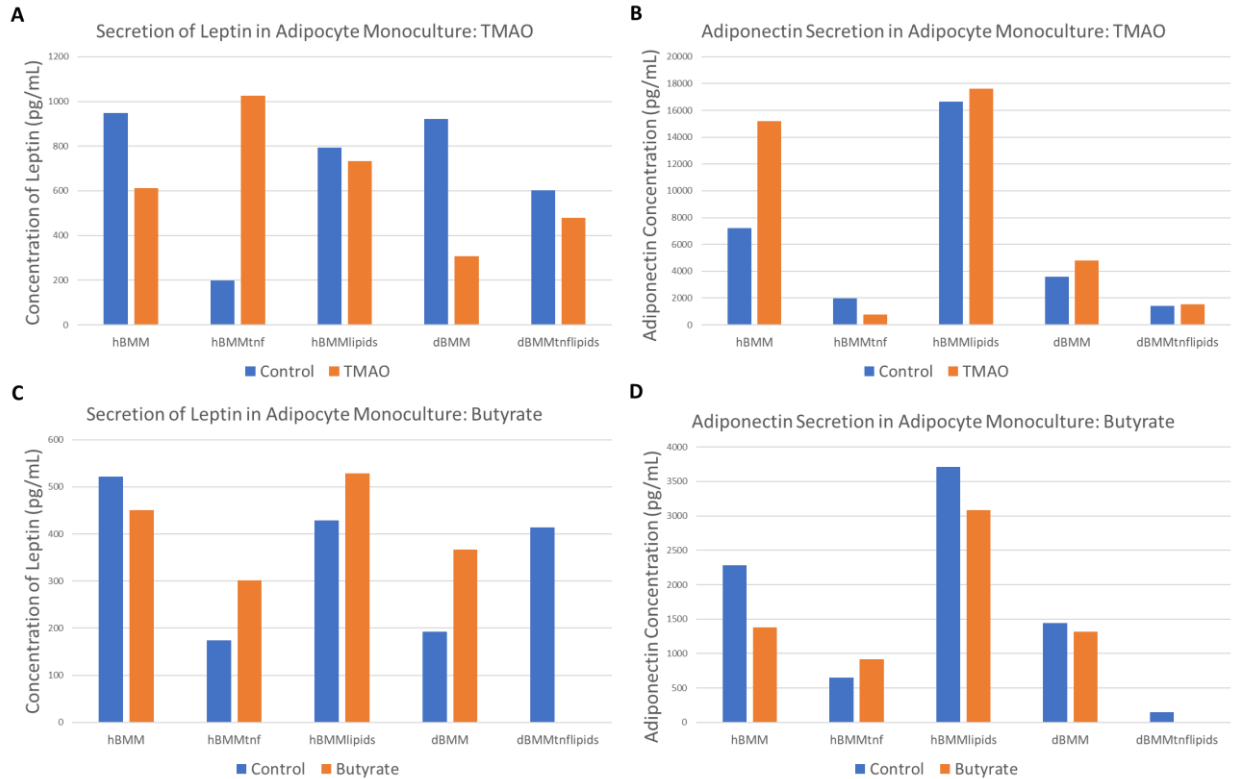
FIGURE 8: Adipocyte Secretion of Cytokines in Monoculture.
*(**A**) Adipocytes were fed for 14 days with hBMM, hBMMtnf, hBMMlipids, dBMM, dBMMtnflipids +/- 10µM TMAO.
On day 14, the concentration of Leptin of the culture supernatant was measured. N=1 for all conditions. (**B**)
Adipocytes were fed for 14 days with hBMM, hBMMtnf, hBMMlipids, dBMM, dBMMtnflipids +/- 10µM TMAO. On
day 14, the concentration of Adiponectin of the culture supernatant was measured. N=1 for all conditions. (**C**)
Adipocytes were fed for 14 days with hBMM, hBMMtnf, hBMMlipids, dBMM, dBMMtnflipids +/- 10µM Butyrate.
On day 14, the concentration of Leptin of the culture supernatant was measured. N=1 for all conditions except
dBMMtnflipids+Butyrate, which was not included. (**D**) Adipocytes were fed for 14 days with hBMM, hBMMtnf,
hBMMlipids, dBMM, dBMMtnflipids +/- 10µM Butyrate. On day 14, the concentration of Adiponectin of the culture
supernatant was measured. N=1 for all conditions except dBMMtnflipids+Butyrate, which was not included.*

FIGURE 9: Expression of GLUT-4 and Insulin Receptor in Monoculture
(**A**) *Adipocytes were fed for 14 days with hBMM, hBMMtnf, hBMMlipids, dBMM, dBMMtnflipids +/- 10μM TMAO. On day 14, the cells were fixed with 4% PFA. Antibodies were used to fluorescently stain for insulin receptor (red) and GLUT-4 (green). Images at 200X were taken using a confocal microscope. N=1 for all conditions.* (**B**) *Adipocytes were fed for 14 days with hBMM, hBMMtnf, hBMMlipids, dBMM, dBMMtnflipids +/- 10μM Butyrate. On day 14, the cells were fixed with 4% PFA. Antibodies were used to fluorescently stain for insulin receptor (red) and GLUT-4 (green). Images at 200X were taken using a confocal microscope. N=1 for all conditions.* (**C**) *The mean grey values of the +/- TMAO images were measured and normalized to hBMM control.* (**D**) *The mean grey values of the +/- Butyrate images were measured and normalized to hBMM control.*

CHAPTER 6: HOAC SYSTEM RESULTS

Culture Health

The MGH hepatocytes in the adipose-liver systems dosed with +/- TMAO were confluent and appeared healthy through 14 days. The adipocytes in the adipose-liver systems dosed with +/- TMAO for 14 days also appeared confluent and healthy. The adipocytes also demonstrated correct morphology, storing lipids. This was true of all three replicates.
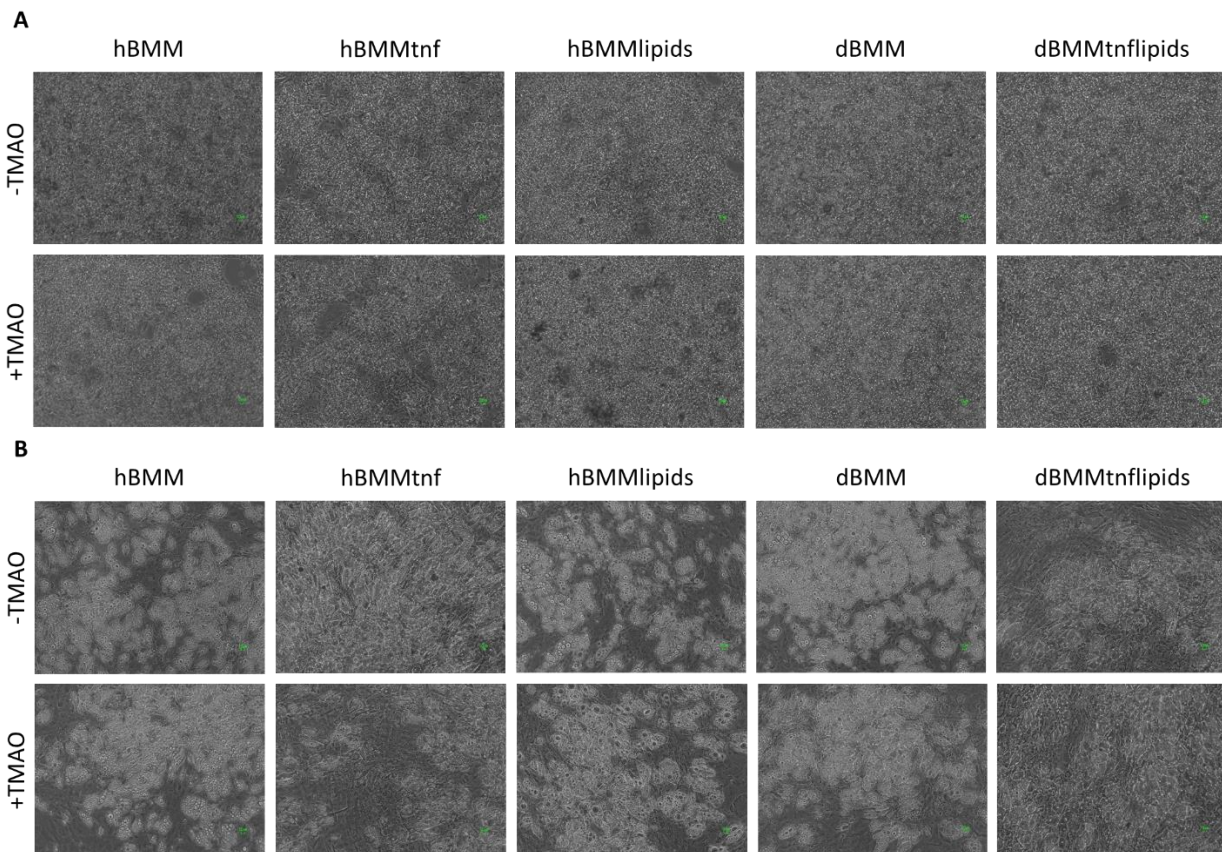
FIGURE 10: Cell Health of Adipose-Liver Systems, TMAO
(A) Adipose-liver systems were fed for 14 days with hBMM, hBMMtnf, hBMMlipids, dBMM, dBMMtnflipids +/-
10μM TMAO. The liver module, containing MGH hepatocytes, was imaged at 100X using a phase microscope. (B)
Adipose-liver systems were fed for 14 days with hBMM, hBMMtnf, hBMMlipids, dBMM, dBMMtnflipids +/- 10μM
TMAO. The WAT module, containing adipocytes, was imaged at 100X using a phase microscope.

The MGH hepatocytes of the adipose-liver systems dosed with +/- Butyrate were

confluent through the endpoint of 7 days. The confluency and health of the cells did appear to

start to decline as day 7 approached. This can be seen most in conditions hBMMtnf and dBMM. The adipocytes of the adipose-liver systems +/- Butyrate were confluent but were not expressing the proper morphology of storing lipids. This suggests that the adipocytes did not differentiate properly for these systems.

The adipose-liver systems +/- Butyrate were cut off at 7 days after previous systems showed signs of toxicity disallowing the hepatocytes to be viable through the 14-day mark. Precautions and extra measures of additional cleaning, medium being remade, and similar efforts were taken to ensure the best health of the cells. The toxicity which was apparent in the previous batches was independent of any factor including butyrate.
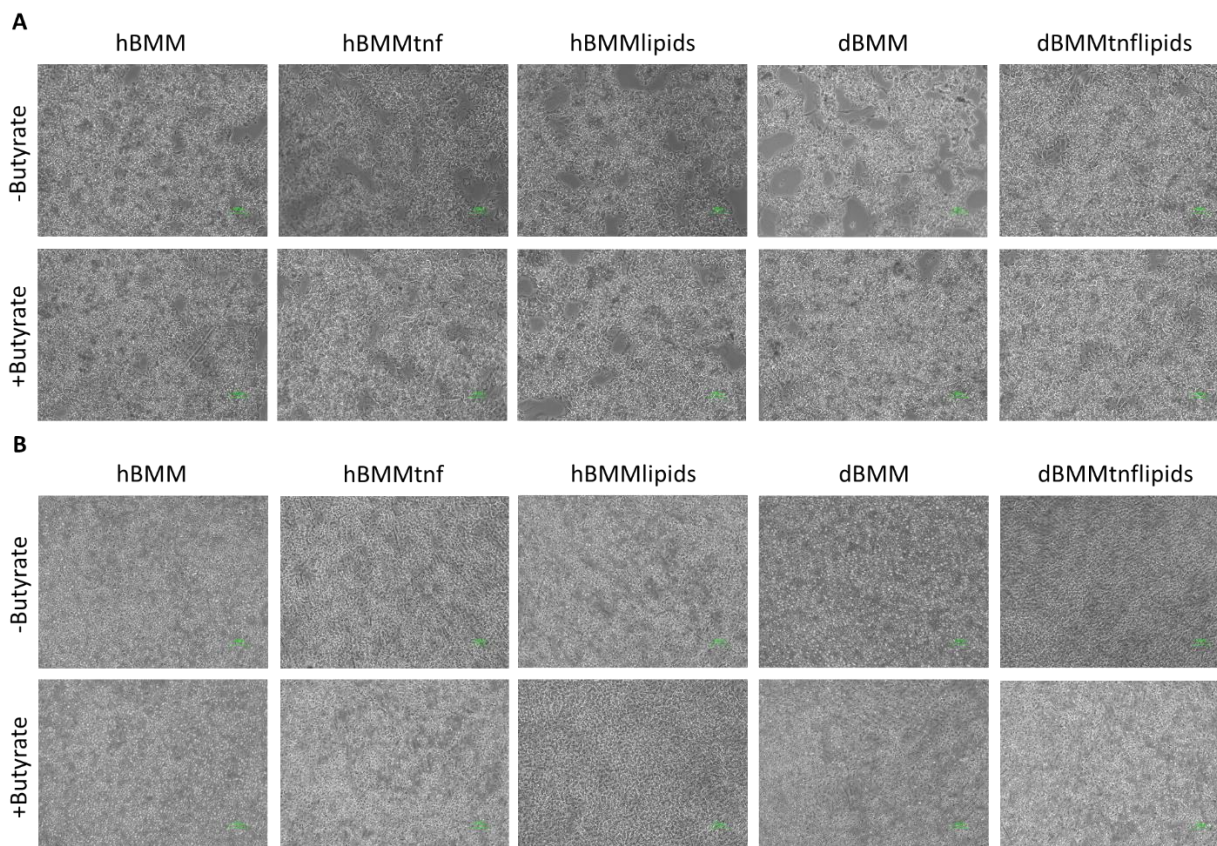
FIGURE 11: Cell Health of Adipose-Liver Systems, Butyrate.
*(**A**) Adipose-liver systems were fed for 7 days with hBMM, hBMMtnf, hBMMlipids, dBMM, dBMMtnflipids +/-*
*10μM Butyrate. The liver module, containing MGH hepatocytes, was imaged at 100X using a phase microscope. (**B**)*
Adipose-liver systems were fed for 7 days with hBMM, hBMMtnf, hBMMlipids, dBMM, dBMMtnflipids +/- 10μM
Butyrate. The WAT module, containing adipocytes, was imaged at 100X using a phase microscope.

Hepatic Steatosis

The MGH hepatocytes in the adipose-liver systems expressed a higher level of steatosis

in the hBMMlipids, dBMM, and dBMMtnflipids +/- TMAO conditions than the hBMM +/-

TMAO. Additionally, steatosis appeared to worsen with TMAO dosing in all conditions

excluding dBMM +/- TMAO.

The hepatocytes in the adipose-liver systems +/- Butyrate expressed worsened steatosis in all conditions compared to the hBMM control through day 7. Butyrate also appeared to improve steatosis in all conditions except for hBMM.
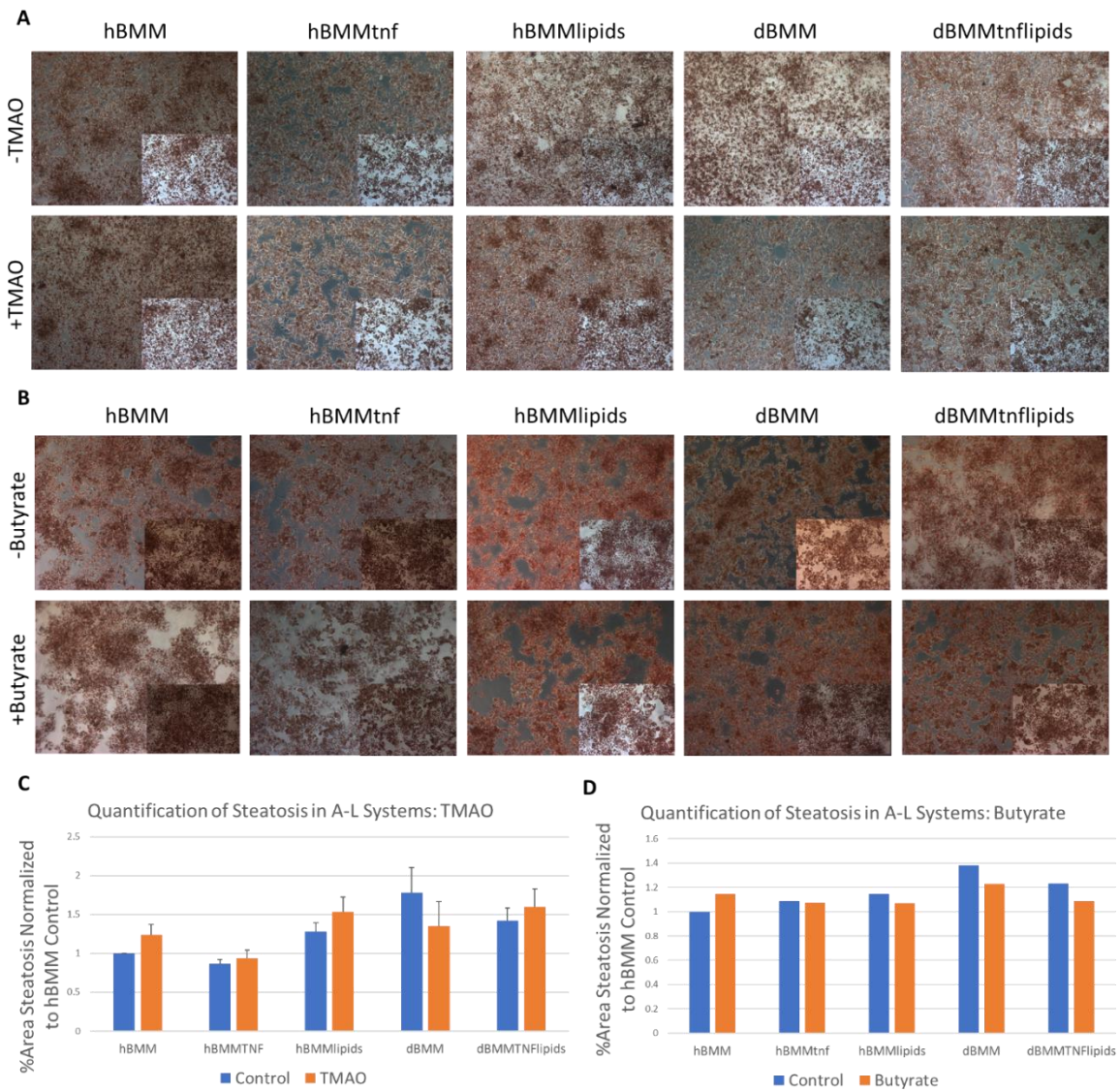
FIGURE 12: Steatosis of Hepatocytes in Adipose-Liver Systems.
(A) Adipose-liver systems were fed for 14 days with hBMM, hBMMtnf, hBMMlipids, dBMM, dBMMtnflipids +/- 10μM TMAO. The liver module, containing MGH hepatocytes, was fixed with 4% PFA and stain with Oil Red O dye. The cells were imaged at 100X and 200X using a phase microscope. (B) Adipose-liver systems were fed for 7 days with hBMM, hBMMtnf, hBMMlipids, dBMM, dBMMtnflipids +/- 10μM butyrate. The liver module, containing MGH hepatocytes, was fixed with 4% PFA and stain with Oil Red O dye. Images were taken at 100X and 200X on a phase microscope. (C) The steatosis expressed in the liver modules +/- TMAO was quantified by taking the %Area of the 200X images using the ImageJ software. The %Area was normalized to the hBMM control. N=3 for all conditions. (D) The steatosis expressed in monoculture hepatocytes +/- Butyrate was quantified by taking the %Area of the 200X images using the ImageJ software. The %Area was normalized to the hBMM control. N=1 for all conditions.

Hepatic Enzyme Activity

As was seen in monoculture, the MGH hepatocytes in the adipose-liver systems +/-
TMAO did not show any CYP3A4 activity in +TNF conditions when measured at 14 days.
Additionally, the dBMM +/- TMAO conditions had more activity than the rest. +TMAO
conditions impaired CYP3A4 activity in all conditions. The hepatocytes from the adipose-liver
systems +/- Butyrate showed limited CYP3A4 activity on day 7. In conditions that had activity,
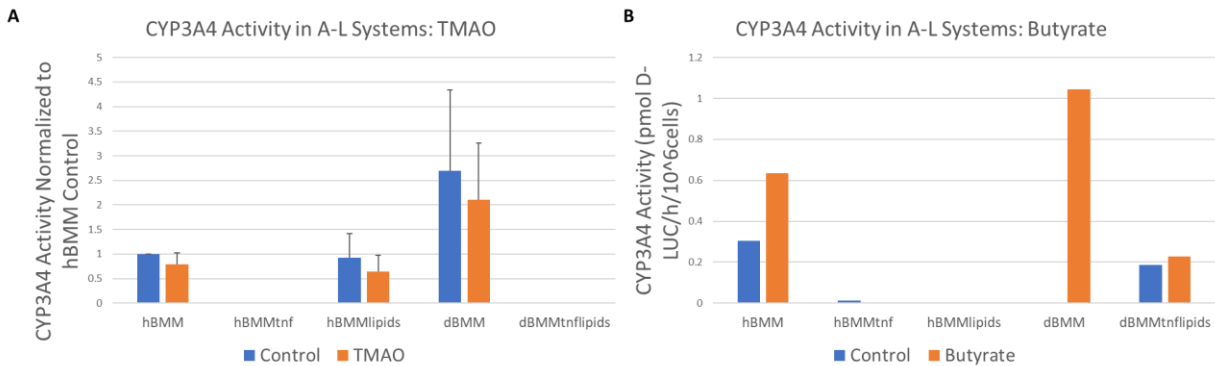butyrate appeared to increase activity compared to controls.

FIGURE 13: CYP3A4 Activity of Hepatocytes in Adipose-Liver Systems.
(A) Adipose-liver systems were fed for 14 days with hBMM, hBMMtnf, hBMMlipids, dBMM, dBMMtnflipids +/-
10μM TMAO. On day 14, the liver module was moved to a 24 well plate and the CYP3A4 activity of the hepatocytes
was measured. N=3 for all conditions. (B) Adipose-liver systems were fed for 7 days with hBMM, hBMMtnf,
hBMMlipids, dBMM, dBMMtnflipids +/- 10μM Butyrate. On day 7, the liver module was moved to a 24 well plate
and the CYP3A4 activity of the hepatocytes was measured. N=1 for all conditions.

Adipocyte Cytokine Secretion and Insulin Resistance

Dosing with TMAO increased the secretion of leptin in adipose-liver systems in most
conditions. The opposite was observed for adiponectin secretion. The expression of GLUT-4 and
insulin receptor in adipose-liver systems decreased in the conditions hBMMlipids +/- TMAO,
dBMM +/- TMAO, and dBMMtnflipids +/- TMAO compared to hBMM control.
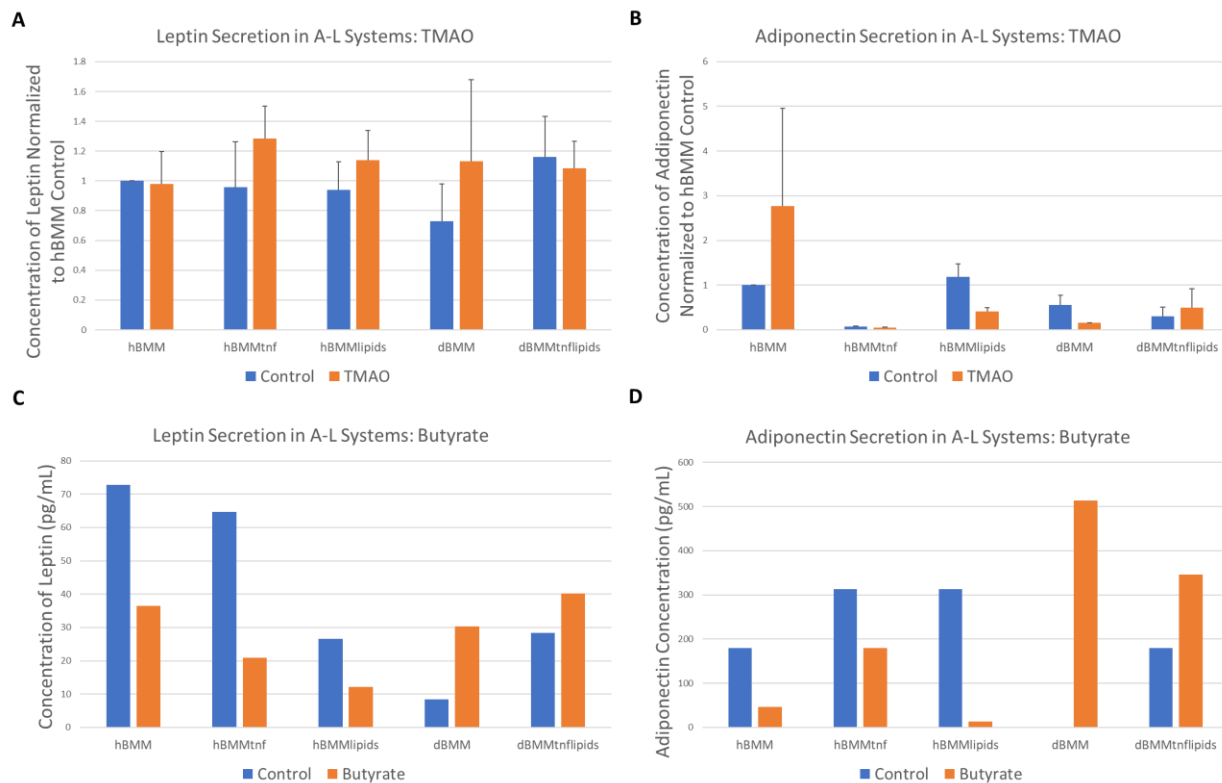
FIGURE 14: Adipocyte Secretion of Cytokines in Adipose-Liver Systems.
(*A*) *Adipose-liver systems were fed for 14 days with hBMM, hBMMtnf, hBMMlipids, dBMM, dBMMtnflipids +/-
10μM TMAO. On day 14, the concentration of Leptin of the culture supernatant was measured. N=3 for all
conditions. (**B**) Adipose-liver systems were fed for 14 days with hBMM, hBMMtnf, hBMMlipids, dBMM,
dBMMtnflipids +/- 10μM TMAO. On day 14, the concentration of Adiponectin of the culture supernatant was
measured. N=3 for all conditions. (**C**) Adipose-liver systems were fed for 7 days with hBMM, hBMMtnf,
hBMMlipids, dBMM, dBMMtnflipids +/- 10μM Butyrate. On day 7, the concentration of Leptin of the culture
supernatant was measured. N=1 for all conditions. (**D**) Adipose-liver systems were fed for 7 days with hBMM,
hBMMtnf, hBMMlipids, dBMM, dBMMtnflipids +/- 10μM Butyrate. On day 7, the concentration of Adiponectin of
the culture supernatant was measured. N=1 for all conditions.*
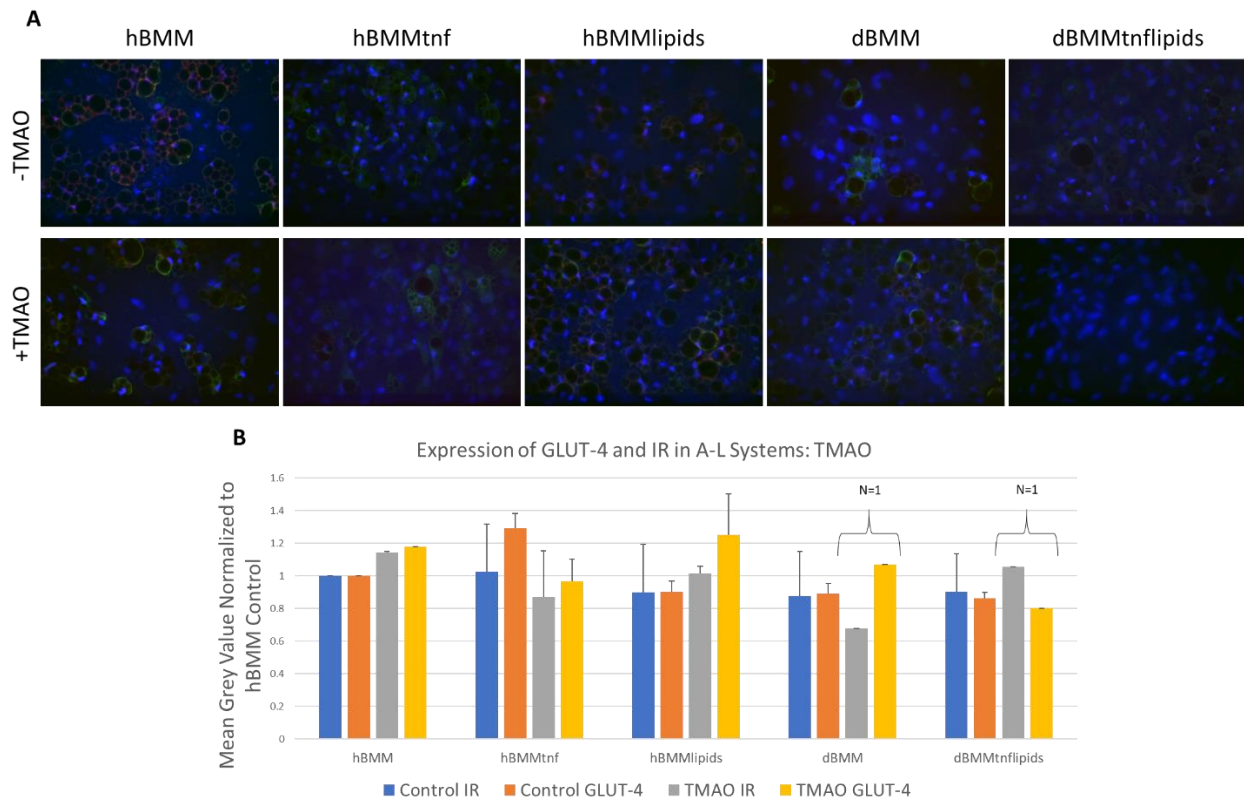
FIGURE 15: Expression of GLUT-4 and Insulin Receptor in Adipose-Liver Systems, TMAO.
(A) Adipose-liver systems were fed for 14 days with hBMM, hBMMtnf, hBMMlipids, dBMM, dBMMtnflipids +/-
10µM TMAO. On day 14, the adipocytes were fixed with 4% PFA. Antibodies were used to fluorescently stain for
insulin receptor (red) and GLUT-4 (green). Images at 200X were taken using a confocal microscope. N=2 for all
conditions except dBMM+TMAO and dBMMtnflipids+TMAO. (B) The mean grey values of the images were
measured and normalized to hBMM control.

CHAPTER 7: DISCUSSION AND CONCLUSION

Adipose-Liver HoaC Systems and NAFLD

A two-organ, adipose-liver, human-on-a-chip, *in vitro* system was used to create a model for non-alcoholic fatty liver disease. This was done using defined medium and human cells; the liver module using primary hepatocytes and the white adipose tissue module using mesenchymal preadipocyte stem cells. By using this kind of novel system, the effects of disease states, the influence of peripheral organs, and impacts of drugs and other compounds can be observed under tightly controlled parameters. Additionally, these systems allow for multiple assays and assay types to be run on the same system.

The potential and utility of these systems is best seen in the adipose-liver systems +/- TMAO. These systems yielded relatively consistent data in several different assays. Although these experiments have not been done in enough replicates to yield statistically significant data at this point, this data and previous data of the characterization of these two-organ systems suggest that a higher throughput study with more replications would have success in testing the effects of various drugs on NAFLD [35].

The main readout for this experiment was the quantification of steatosis. With the exception of the hBMMtnf +/-TMAO conditions, all conditions displayed higher amounts of steatosis than the hBMM control (Figure 12). Since the disease states of obesity and diabetes are correlated with NAFLD, it not surprising that the same would be true in adipose-liver systems. It is important to note that this trend was seen in not only the adipose-liver systems +/- TMAO, but in the adipose-liver systems +/- Butyrate and the two monocultures as well (Figures 6, 12).

Another important observation is the effect that TNF-α had on the cultures. In the adipose-liver systems +/- TMAO, the hBMMtnf +/- TMAO stored less lipids than the hBMM control. Similarly, the dBMMtnflipids +/- TMAO conditions were lower in steatosis than the dBMM condition, which was unexpected (Figure 12). The most likely explanation for this is that the TNF-α was causing cell death and thus the cultures themselves were less confluent and so the overall steatosis was less while the steatosis per cell could have potentially been higher. This explanation is supported qualitatively by the images and quantitatively by the CYP3A4 activity. In the +/- TMAO systems, the +/- Butyrate systems, and both monocultures, the hBMMtnf +/- TMAO/Butyrate and dBMMtnflipids +/- TMAO/Butyrate conditions had almost no CYP3A4 activity (Figures, 7, 13). This indicates that the hepatocytes' functionality was greatly reduced when dosed with TNF-α. There are two potential reasons behind this: the first is that the concentration dosage was too high and thus was toxic to the cells. The other option is that the TNF- α was causing the hepatocytes to progress in the NAFLD disease spectrum. As was mentioned before, NAFLD can progress to disease states such as NASH, fibrosis, and eventually cancer. TNF-α could be causing the damage necessary for the progression to disease states such as fibrosis which cannot be modeled in this specific HoaC system.

In the CYP3A4 assay, the conditions of dBMM+/- TMAO displayed more activity than the hBMM control (Figure 13). This was originally unexpected but can be explained by the fact that the additional glucose, although worsening the steatosis, could be acutely making the cells more metabolically active.

Although there are some patterns emerging in the quantification of leptin and adiponectin, with the limited data set, it is difficult to make any conclusions as to the role of the

various conditions in adipose health (Figures 8, 14). Similarly, it is not possible at this time to determine the adipocytes' role in NAFLD progression in the liver until further monoculture and adipose-liver system replicates are completed.

In most conditions in the adipose-liver systems, there was less expression of GLUT-4 and insulin receptor compared to the hBMM control (Figure 15). This is an expected result and further demonstrates that in the adipose-liver HoaC model the expected phenotypes of NAFLD can be emulated. The adipose-liver HoaC systems show a promising start to the modeling of NAFLD. Each batch of these systems can yield a great deal of data. HoaC systems, specifically the adipose-liver two organ systems, are new and cutting-edge innovations. As with any novel technology, it is inevitable that there will be hurdles to overcome.

An example of this was the occurrence of toxicity in some of the systems. The reason why the adipose-liver systems +/-Butyrate were limited to 7 days instead of the intended 14 was that previous +/-Butyrate systems had some toxicity. The toxicity was remedied by a change in the cleaning protocol of the housings, but a shorter dosing was used due to time limitations and to ensure the systems' success.

The cells themselves offer a challenge. Eukaryotic, specifically human, cells tend to take a long time to culture and can be difficult to work with. These systems each represent a month, from the plating of the adipocytes to the disassembly of the systems. In a high throughput, standardized study, with the human and physical resources to tightly overlap batches, this is not a significant hurdle. However, this does speak to the limitations of these systems; their physiological relevance, controlled parameters, and versatility of assays comes with a higher cost of failure. But it is important to note, that as these systems are used more, with unsuccessful

batches occurring periodically, they and their usage will be better characterized and altered towards a reliable, physiologically relevant, *in vitro* model for disease which could redefine drug testing.

The Gut Microbiome's Role in NAFLD

There were a couple of notable trends observed regarding the gut microbiome's role in NAFLD. The first of which was that TMAO does appear to worsen steatosis in the liver in the adipose-liver systems. This was seen in all conditions except dBMM. The opposite was true of butyrate which lowered steatosis in the adipose-liver systems in all conditions except hBMM (Figure 12). These results, that TMAO would increase steatosis while butyrate would decrease it, were the expected results based on the literature. However, these results were not seen in monoculture (Figure 6). It is unclear at this time whether this is due to the adipocytes' influence in the HoaC systems or if it is due to the limited number of replicates. The hypothesis that TMAO would worsen disease states was also supported by the CYP3A4 activity. In each condition, TMAO decreased CYP3A4 activity in the HoaC systems (Figure 13). Butyrate increased CYP3A4 activity in the adipose-liver systems, which would suggest that butyrate improves liver function (Figure 13).

As was mentioned previously, although NAFLD is highly correlated with obesity and type II diabetes, there are still cases of NAFLD in otherwise healthy individuals. The hypothesis was thus put forward that a dysbiosis of the gut microbiome could account for this subset of the population. TMAO's effects in hBMM adipose-liver systems supports this idea. TMAO in hBMM adipose-liver systems both increases steatosis and decreases CYP3A4 activity (Figures

12, 13). It is thus possible that an increase in choline metabolizing microbiota would induce NAFLD in otherwise healthy individuals.

Similarly, butyrate increased steatosis in hBMM, in both monoculture and adipose-liver systems, while decreasing steatosis in most other conditions (Figures 6, 12). If this pattern continues in additional replicates, it would highlight another potential mechanism by which the GM can influence NAFLD in otherwise healthy patients. While butyrate's beneficial anti-inflammatory properties normally operate to decrease steatosis in disease states, butyrate can also function as an energy source. If butyrate levels in the liver were increased, due to dysbiosis or leaky gut syndrome, the liver could end up storing this excess energy source as lipids.

Increased leptin and decreased adiponectin were observed in the hBMMtnf, hBMMlipids, dBMM conditions when dosed with TMAO in the adipose-liver systems. The opposite was seen for the hBMM and dBMMtnflipids conditions (Figure 14). It is possible that the change in cytokine secretion was a response to the stimulus of TMAO by the adipose module to protect the liver module from the inflammatory properties of TMAO. If this is true, it would highlight adipocytes protective function in disease progression. Further replicates would allow for this hypothesis to be more fully explored. At this point, there is not enough data to determine the effects of the gut microbiome on adipocyte expression of GLUT-4 and insulin receptor.

Further experimentation is necessary to solidify and identify by what mechanisms the GM may be impacting liver health. Future experiments could take the direction of additional replicates but could also be expanded to allow an even more holistic model of the GM and NAFLD. In the current experiments, the cultures were dosed with singular compounds. In future experiments, supernatant from live bacteria, cultured in different conditions, could be used to

dose the systems instead. Colon health and permeability is a major factor in the transport of compounds to the liver. Therefore, an additional module for the colon would incorporate another important aspect of NAFLD progression.

Conclusion

Using the HoaC systems, the effects of the gut microbiome have started to be elucidated. This initial data is supportive of the hypothesis that a dysbiosis of the GM can influence the pathogenesis of NAFLD. More importantly, these experiments have added to the utility and development of human-on-a-chip systems. Despite some difficulty in early experiments, the adipose-liver, two-organ systems have significant potential in the testing of drugs and for the modeling of disease.

REFERENCES

1. Buzzetti, E., M. Pinzani, and E.A. Tsochatzis, *The multiple-hit pthogenesis of non-alcoholic fatty liver disease (NAFLD).* Metabolism Clinical and Experimental, 2015. **65**: p. 1038-1048.
2. Michelotti, G.A., M.V. Machado, and A.M. Diehl, *NAFLD, NASH and liver cancer.* Mat. Rev. Gastroenterol. Hepatol., 2013. **10**: p. 656-665.
3. Christopher D, W., et al., *Prevalence of nonalcoholic fatty liver disease and nonalcoholic steatohepatitis among a largely middle-aged population utilizing ultrasound and liver biopsy: A prospective study.* Gastroenterology, 2011(140): p. 124-131.
4. Charlton, M.R., et al., *Frequency and outcomes of liver transplantation for nonalcoholic steatohepatitis in the United States.* Gastroenterology, 2011. **141**: p. 1249-1253.
5. Fang, Y.-L., et al., *Pathogenesis of non-alcoholic fatty liver disease in children and adolescence: From "two hit theory" to "multiple hit model".* World Journal of Gastroenterology, 2018. **24(27)**: p. 2974-2983.
6. Ferramosca, A. and V. Zara, *Modulation of hepatic steatosis by dietary fatty acids.* World Journal of Gastroenterology, 2014. **20(7)**: p. 1746-1755.
7. George, J. and C. Liddle, *Nonalcoholic fatty liver disease: pathogenesis and potential for nuclear receptors as therapeutic targets.* Molecular Pharmaceutics, 2007. **5**: p. 49-59.
8. Tsochatzis, E.A., G.V. Papatheodoridis, and A.J. Archimandritis, *Adipokines in nonalcoholic steatohepatitis: from pathogenesis to implications in diagnosis and therapy.* Mediators of Inflammation, 2009: p. 1-8.
9. Wullaert, A., et al., *Hepatic tumor necrosis factor signaling and nuclear factor-kB: effects on liver homeostasis and beyond.* Endocrine Reviews, 2007. **28(4)**: p. 365-386.
10. Hotamisligil, G.S., *Inflammation and metabolic disorders.* Nature, 2006. **444**: p. 860-867.
11. Zhu, L., R.D. Baker, and S.S. Baker, *Gut microbiome and nonalcohoolic fatty liver diseases.* Pediatric Research, 2015. **77**: p. 245-511.
12. Sender, R., S. Fuchs, and R. Milo, *Are we really vastly outnumbered? Revisiting the ratio of bacterial to host cells in humans.* Cell, 2016. **164**: p. 337-340.
13. Grabherr, F., et al., *Gut dysfunction and non-alcoholic fatty liver disease.* Frontiers in Endocrinology, 2019. **10**.
14. Caspani, G., et al., *Gut microbial metabolites in depression: understanding the biochemical mechanisms.* Microbial Cell, 2019. **6**.
15. Nie, J., et al., *Serum trimethylamine n-oxide concentration is positively associated with first stroke in hypertensive patients.* Stroke, 2018. **49**: p. 2021-2028.
16. Duarte, S.M.B., et al., *Gut microbiome composition in lean patients with NASH is associated with liver damage independent of caloric intake: a prospective pilot study.* Nutrition, Metabolism & Cardiovascular Diseases, 2018. **38**: p. 369-384.
17. Chu, H., B. Williams, and B. Schnabl, *Gut microbiota, fatty liver disease, and hepatocellular carcinoma.* Liver Research, 2018: p. 1-9.
18. Shen, F., et al., *Gut microbiota dysbiosis in patients with non-alcoholic fatty liver disease.* Hepatobiliary Pancreat Dis Int, 2017. **16**: p. 375-381.
19. Craciuin, S. and E.P. Balskus, *Microbial conversion of choline to trimethylamine requires a glycyl radical enzyme.* PNAS, 2012. **109**: p. 21307-21312.
20. Ridlon, J.M., et al., *Bile acids and the gut microbiome.* Current Opinion Gastroenterol, 2014. **30(3)**: p. 332-338.

21.   Mokhtari, Z., D.L. Gibson, and A. Hekmatdoost, *Nonalcoholic fatty liver disease, the gut microbiome, and diet.* Adv Nutr, 2017. **8**: p. 240-252.

22.   Chen, Y.-m., et al., *Associations of gut-flora-dependent metabolite trimethylamine-N-oxide, betaine and choline with non-alcoholic fatty liver disease in adults.* Scientific Reports, 2016.

23.   Koeth, R.A., et al., *Intestinal microbiota metabolism of L-carnitine, a nutrient in red meat, promotes atherosclerosis.* Nat Med, 2013. **19(5)**: p. 576-585.

24.   Bloemen, J.G., et al., *Short chain fatty acids exchange across the gut and liver in humans measured at surgery.* Clinical Nutrition, 2009. **28**: p. 657-661.

25.   Canani, R.B., et al., *Potential beneficial effects of butyrate in intestinal and extraintestinal diseases.* Gastroenterology, 2011. **17(12)**: p. 1519-1528.

26.   Gao, Z., et al., *Butyrate improves insulin sensitivity and increases energy expenditure in mice.* Diabetes, 2009. **56**: p. 1509-1517.

27.   Akhtar, A., *The flaws and human harms of animal experimentation.* Cambridge Quarterly of Healthcare Ethics, 2015. **24**: p. 407-419.

28.   Meer, P.J.K.c., M.L. Graham, and H.-J. Schuurman, *The safety, efficacy and regulatory triangle in drug development: impact for animal models and the use of animals.* European Journal of Pharmacology, 2015. **759**: p. 3-13.

29.   Taylor, K., et al., *Estimates for worlwide laboratory animal use in 2005.* ATLA, 2008. **36**: p. 327-342.

30.   Bhatia, S.N. and D.E. Ingber, *Microfluidic organs-on-chips.* Nature Biotechnology, 2014. **32**: p. 760-772.

31.   Wang, Y.I., et al., *Multiorgan microphysiological systems for drug development: strategies, advances, and challenges.* Advanced Healtthcare Materials, 2017. **7**.

32.   CarlotaOleaga, et al., *Multi-organ toxicity demonstration in a functional human in vitro system composed of four organs.* Scientific Reports, 2016. **6**.

33.   Esch, E.W., A. Bahinski, and D. Huh, *Organs-on-chips at the frontiers of drug discovery.* Nat Rev Drug Discovery, 2015. **14(4)**: p. 248-260.

34.   Moffat, J.G., et al., *Opportunities and challenges in phenotypic drug discovery: an industry persective.* Nat Rev Drug Discovery, 2017. **16**.

35.   Slaughter, V., et al., *Development and characterization of a two-organ human-on-a-chip NAFLD model*, in *Integrated Pathways of Disease in NASH and NAFLD*. 2019: Santa Fe, New Mexico.

36.   Rueden, C.T., et al., *ImageJ2: ImageJ for the next generation of scientific image data.* BMC Bioinformatics, 2017. **529**.